Cross shelf transport introduced by the Lofoten Maelstrom

A. Ommundsen
Department of Mathematics, University of Oslo
P.O.Box 1053 Blindern, Oslo, Norway

June 17, 1999

Abstract

Drift of particles released in the tidal current (Moskstraumen) near Lofotodden, located at 67°50′N, 12°50′E, is studied. The periodical tidal current combined with a background current is found to introduce a transport between Vestfjorden inside Lofotodden and the shelf outside. This transport may be important for drift of cod eggs, larvae and other important biological and chemical tracers.

A fine-resolution numerical model provided the Eulerian tidal current field. Based on this current field the particle trajectories is calculated using a Lagrangian particle tracking technique. The tracking algorithm was extended by a random-walk method to simulate small scale turbulence. An idealized current model of the area is also developed. This model is used as a simplification tool revealing the basic mechanisms of the drift and to demonstrate the sensibility of time stepping in numerical integration.

1 Introduction

To make scientific well judged decisions regarding the resources along the coast of Norway, better knowledge about how the tide influences the local ocean environments is needed. Periodic tidal variations in the ocean surface dominate other oceanographic signals, and the tidal currents will represent an important part of the overall current field. Tidal currents commonly of order 1 m/s may be significantly increased when constrained by topography. The famous tidal current Moskstraumen, also known as the Lofoten Maelstrom, outside Lofotodden is an example, running with strength up to 3-5 m/s.

In an earlier work by Gjevik et al. (1997), a fine resolution numerical model for the tide around Lofoten was developed. The domain of this model is depicted in figure 1. The article documented high difference in the sea level in the sound between Lofotodden and Værøy, with the small island Mosken in the middle (figure 1, right panel). The maximum strength of Moskstraumen was estimated to be approximately 3 m/s for the M_2 component. With the tidal current data from Gjevik et al. (1997) and idealized background currents (BC), we have studied horizontal particle drift in Moskstraumen. The particle tracking algorithm in this report is similar to the method used by Gjevik (1996) to simulate particles drift in the tidal flow in other regions along the Norwegian coast. The periodic tide combined with the steady BC in the area is shown to be an important mechanism for exchanging water-masses between Vestfjorden and the open sea. Although this study primary focuses on a particular application, similar mechanism for cross shelf transport can be important in other areas. The results of this study may therefore be of a wider interest.

Numerous papers concerning particle drift and dispersion in the ocean and atmosphere exist. In these papers several solution methods are proposed. The paper by Turell (1994)

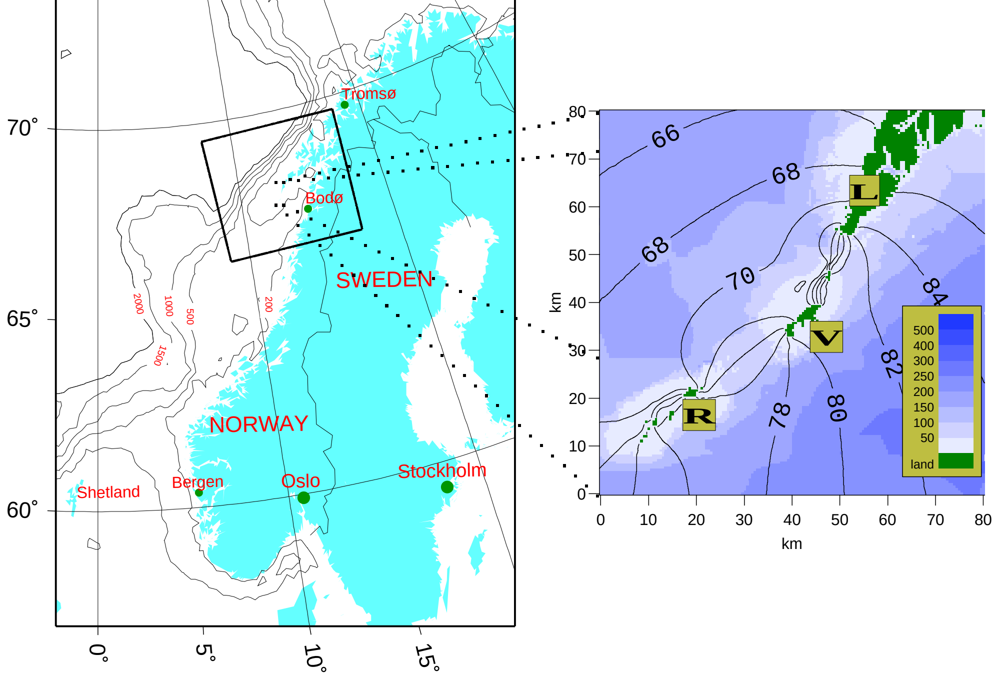

Figure 1: Square box in left panel shows the location of Lofoten and the total model domain. Lofoten is located on the northern Norwegian continental shelf (left). Vestfjorden lies inside the Lofoten archipelago northwest of Bodø. Right panel: Enlarged map of the area near Lofotodden. The labels are; Lofotodden (L), Værøy (V) and Røst (R). Color depth scale in meters (legend), and contour lines for amplitude with equidistant 2 cm for the M_2 tidal constituent.

reviews some of the numerical modelling efforts that took place during the days following the grounding of the tanker *Braer*. Several organizations participated in the development of numerical models predicting the oil spill, which was initially located at the tip of Shetland Island. These models were repeatedly compared to data. The conclusion was that forecasting movement of oil and water under action of tide and wind may be accomplished using computer models and the need for higher spatial resolution was stressed. Due to severe weather conditions the necessary model parameters, derived from measurements at sea, were unreliable and difficult to obtain. This combined with the need to develop new or to improve existing numerical models during the propagation of the spill made forecasting unreliable.

The largest deliberate oil spill, 25 km south of Kuwait City in 1991, is modeled in the article by Proctor^2 et al. (1994). Controlled and legal releases of oil was made in the North Sea, and the observed drift was used to validate a numerical model discussed in Elliott et al. (1986) and Elliott (1986). These models used Lagrangian particle tracking and the random-walk technique instead of the more classic advection-diffusion equation approach.

The importance of residual currents are discussed in the articles by Zimmerman (1986), Ridderinkhof and Zimmerman (1992) and Geyer and Signell (1992). A nonlinear tidal model will introduce residual currents which may exhibit considerably variability over the length of the tidal excursion (i.e. the horizontal displacement of fluid particles). This perturbation of the basic oscillatory flow can generate chaotic particle motions, in that particles released at nearby positions at a special moment follow strongly divergent pathways in later times.

In this report the complex drift of particles released are due to gradients in the Eulerian current field and the net transport is caused by the interaction between the oscillatory tidal flow and the steady background current. The background current in the area is much larger than the tidal residual current, so in this study the latter was neglected. A random-walk algorithm was also implemented to simulate turbulence on small scale. The effect and reliability of this algorithm is strongly connected to the choice of diffusion coefficients. In Elliott et al. (1992), Elliott (1986) and Proctor[2] et al. (1994) the random-walk technique is used with different models for the diffusion coefficient.

The north-west part of Vestfjorden is an important spawning area for the Arcto-Norwegian cod during March and April (Ellertsen et al. 1980). Moskstraumen, combined with the general circulation, should therefore be an important actor in the transport of cod eggs, larvae etc between Vestfjorden and the open ocean. Simulations of particles studied in this report indicates horizontal drift and dispersion of zooplankton, eggs, pollution etc. These quantities are treated as passive particles drifting with flow, assuming swimming and migration of minor importance.

2 Equation for particle motion

The high-resolution tidal model of (Gjevik et al. 1997) provides time series of currents and sea level with a spatial resolution of 500 meters. These simulations are made with a depth-integrated linear model (the bottom-friction is nonlinear). A harmonic analysis of these time series provides the harmonic constants for the depth mean currents. With a horizontal Cartesian coordinate system, origin at left lower corner and x, y axes along the model domain (figure 1), the x and y components of the M_2 depth mean current velocity are represented respectively as

$$\begin{aligned} u(x,y,t) &= U\cos(\omega t + \chi - \delta_u) \quad (1) \\ v(x,y,t) &= V\cos(\omega t + \chi - \delta_v) \quad (2) \end{aligned}$$

Here (U, V) denotes the amplitudes, ω the angular velocity, (δ_u, δ_v) the phases relative to Greenwich and χ the astronomical argument. The current field due to other tidal components may be included in the expressions (1) and (2); see Gjevik (1996). With a nearly linear tidal model and approximation (1)-(2), we neglect the effect of tidal driven residual currents.

Lagrangian motion of particles is found by integrating the equations

$$\frac{dx_k}{dt} = u(x_k, y_k, t) \qquad \frac{dy_k}{dt} = v(x_k, y_k, t) \quad (3)$$

Subscript k denotes the number of a single particle ($k = 1 \dots M$, M = number of particles) and (x_k, y_k) its position.

3 Numerical method and accuracy

We have used a forth order Runge-Kutta method as initiator combined with an Adam-Moulton method for the numerical integration of the equations (3). This combination will reduce the computer time, still keeping a truncation error of Δt^5 (e.g. Boyce and DiPrima (1992)).

In the idealized model, described in section 4, the current is provided by an analytical formula and the current field is hence described for all location in time and space. In the Lofoten model however, described in section 5, the data originate from a finite difference method and are therefore discontinuous. We therefore use a bilinear interpolation routine between 4 spatial grid points to generate the information needed in between the finite difference grid points. In each grid point the current is continuous in time due to the representation given by equations (1) and (2). The use of unmodified bilinear interpolation is source to unwanted effects near land. Nearest neighbour interpolation, which returns the value of the closest grid point, was therefore used if the nearest neighbour had zero velocity. Particles are "beached" when they encounter a dry grid cell. There are numerous ways to treat beached particles, e.g. Proctor^1 et al. (1994), Proctor^2 et al. (1994). In our simulations beached particles are deadlocked for the rest of the simulation.

Unreliable trajectories and even on-shore drift of particles is the consequence of using too large time step in the numerical integration. A sufficiently small enough time step ensure that no particles move more than a fraction of a grid cell in one time step. In these simulations the convergence of the particle path with decreasing time step was used to find an appropriate time step, see discussion subsection 4.1.

By solving the equations (3) we can simulate advection to a high degree of accuracy. The dispersion of a passive substance within such a fluid is not resolved by the advection alone. Turbulence will contribute to a randomly displacement of the particles released. The Lagrangian particle-tracking technique simulate turbulent diffusion effectively by the use of a 'random-walk' method (Hunter 1987).

We define a diffusion length

$$D = R_1\sqrt{12K_h\Delta t} \tag{4}$$

where R_1 is a random number drawn from a uniform distribution between 0 and 1 and K_h is the diffusion coefficient. The position of a particle was then calculated by numerical integration of the equations (3) combined with a displacement of length D each time step. The direction of the displacement D was set by the angle $2\pi R_2$, where R_2 is a random number also drawn from a uniform distribution between 0 and 1.

Homogeneous diffusion on a small scale is modeled by a constant diffusion coefficient K_h. This random method alone is then a simulator of Fickian dispersion where the corresponding effective diffusivity, K, is given by

$$K = \frac{1}{2}\frac{d\sigma^2}{dt} \tag{5}$$

Here σ is the variance of the particle distribution calculated in any direction. The scaling of the diffusion length D combined with the direction of displacement $2\pi R_2$, provide a diffusion coefficient K_h which equal the effective diffusivity K. Equation (5) can be obtained by investigating the mass (zeroth moment), center of mass (first moment) and the variance (second moment) deduced from the diffusion equation. Furnes (1994) analyzed these moments and also demonstrated the close resemblance between the solution of the random method and the diffusion equation for available analytical solutions of the diffusion equation. With a constant diffusion the center of mass will not change in time and the variance is proportional the diffusion. A gradient in the diffusion will cause the centroid to move in direction of stronger diffusivity. Results with the diffusion term active is provided in section 6.

4 An idealized model

It is of interest to first study particle motion in an idealized model. This idealized model captures important dynamics of the current field near Lofotodden. Such a model enables a more controllable model environment, and reveals the basic mechanism for the exchange between Vestfjorden and the outer shelf.

The model geometry is shown in figure 2. The model domain consist of two impenetrable walls, representing respectively Lofotodden and the island chain south of Værøy. Although the numerical model implements these walls with an infinitely small width, they are drawn with an artificial extension in the figures. An aperture of b = 16 km separate these walls, which is approximately the true distance between Værøy and Lofotodden. In this simple model these walls are infinite on both sides of the aperture.

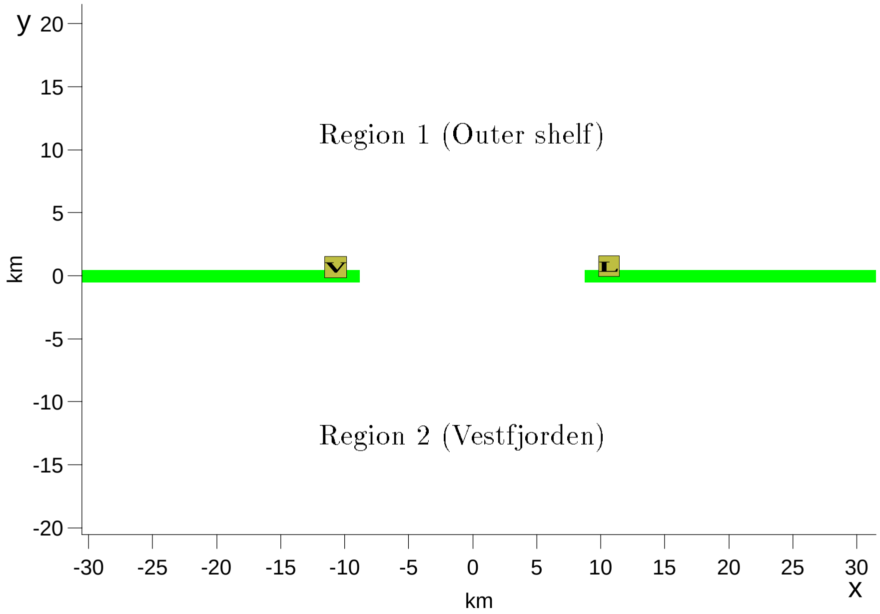

Figure 2: Two solid, impenetrable walls represent respectively Værøy (V) and Lofotodden (L). The outer shelf is marked as region 1 ($y > 0$), while Vestfjorden is marked as region 2 ($y < 0$).

Moskstraumen is simulated by a flow trough an aperture (Milne-Thomson 1968, page 158). The equation for this flow is

$$\frac{x^2}{c^2\cos^2(\alpha\psi)} - \frac{y^2}{c^2\sin^2(\alpha\psi)} = 1 \tag{6}$$

Here ψ denotes the stream function. Streamlines $\psi =$ constant are confocal hyperbolas, with foci $(-c, 0), (c, 0)$. The speed at these foci will be infinite, thus our aperture must be chosen $b < 2c$. We chose c to be 10 km and $b = 16$ km. Streamlines that intersects the x-axis outside our aperture ($|x| > 8$) are naturally excluded. The parameter α controls the strength of the current. The flow is multiplied with $\cos(\frac{2\pi}{T}t - \delta)$, $T = 12.4$ hours, to provide the oscillation of the M_2 tidal current. The phase δ is included to control the initial direction and strength of this flow. The velocity profile between the coordinates $(\pm 8, 0)$ is a parabola with maximums close to the walls. This profile roughly models the current increase in shallow water close to land compared to more weaker currents at deeper depths in the middle. The current speed in the aperture was chosen to approximate the modeled current in Moskstraumen. A maximum value of the current in Moskstraumen was estimated to be about $2 - 3$ m/s (Gjevik et al. 1997) during one tidal cycle. We scaled the model so that the strength in the middle of the aperture (origin) was $v_0 = 1.5$ m/s in the y-direction which gave a maximum value of 2.5 m/s in the y-direction at the edges of the aperture ($\alpha = 6.6672 \cdot 10^{-5}$).

Figure 3 displays the corresponding flow field. A region, shaped like a double axe, is drawn onto this figure. Inside this region tidal excursion is sufficiently large to displace particles through the aperture. The extension and shape of this scallop depends on the velocity v_0, the value of foci c and the period T.

Steady background currents (BC), with different magnitude and in opposite direction in the two regions, are superimposed to this flow. In region 1 and 2 the BC are denoted respectively $\vec{U_1}$ and $\vec{U_2}$. The BC are smoothed as tanh, this to avoid discontinuity in the aperture

$$\vec{U_1} = |C_1|\tanh(\frac{y}{R})\vec{i} \qquad \vec{U_2} = -|C_2|\tanh(\frac{|y|}{R})\vec{i} \tag{7}$$

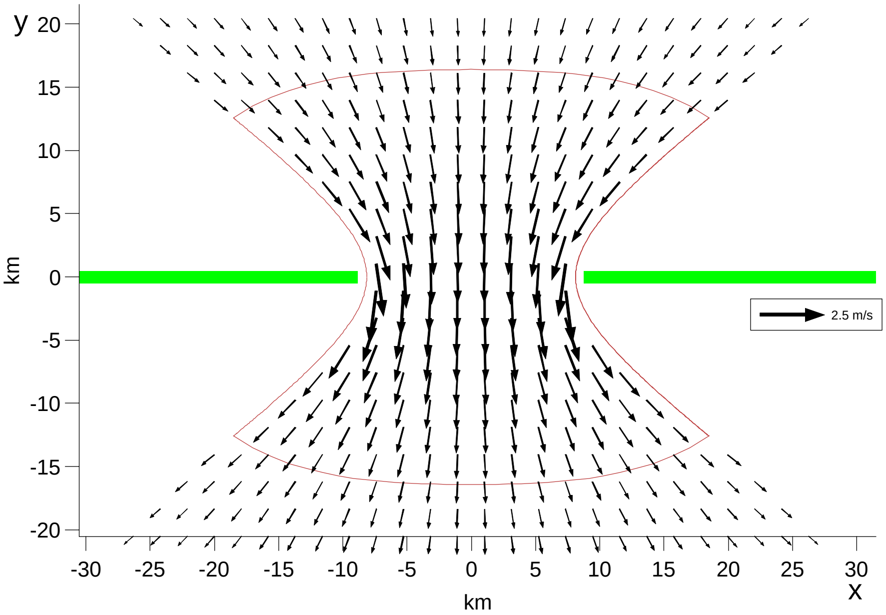

Figure 3: Sketch of the velocity through the aperture. The vectors represents the strength of the current. Streamlines are hyperbolas with foci $(-10, 0), (10, 0)$. The outermost streamline intersects the x-axis in $(\pm 8, 0)$. In this figure $t = 0$ and the phase is set to zero.

Here C_1, C_2 are the strengths of the BC and R the smoothing length. The vector $\vec{i}$ is the unit vector pointing in positive x-direction. Figure 4 shows the current field with BC superimposed.

In table 1 we have listed the essential fixed parameters and variables in this model. The variables, which will be studied more throughly are marked *var*. A function P of the variables C_1, C_2, R, x and y, which measure the exchange of particles, can be defined as:

$$P = \frac{\textit{Number of particles changing region}}{\textit{Total number of particles dropped in position x,y}} \tag{8}$$

In the number of particles *changing region* in equation (8) only particles that leave their initial region permanently are counted. We here refer to P as the exchange parameter.

Table 1: Key parameters and variables for the idealized model

b	Width of the aperture	16 km
v_0	Strength of the current in origin	1.5 m/s
T	Period of the tide (M_2)	12.4 hour
c	Foci of the hyperbolas	10 km
(x, y)	Location where particles are dropped	*var*
C_1	Strength of BC region 1	*var*
C_2	Strength of BC region 2	*var*
R	Smoothing length	*var*
δ	The phase of the oscillatory term	*var*

The exchange parameter P is a function of the variables C_1, C_2, R and y upstream in region 1 and 2. As $|y|$ increase from the walls, P decrease and will be zero for $y \geq L_1$ in region 1 and $|y| \geq L_2$ in region 2. P is a concave downward function of y. In a simulation of P, represented by figure 9, we estimate L_1 to be 8 km and L_2 to 13 km. Altering C_1 and C_2

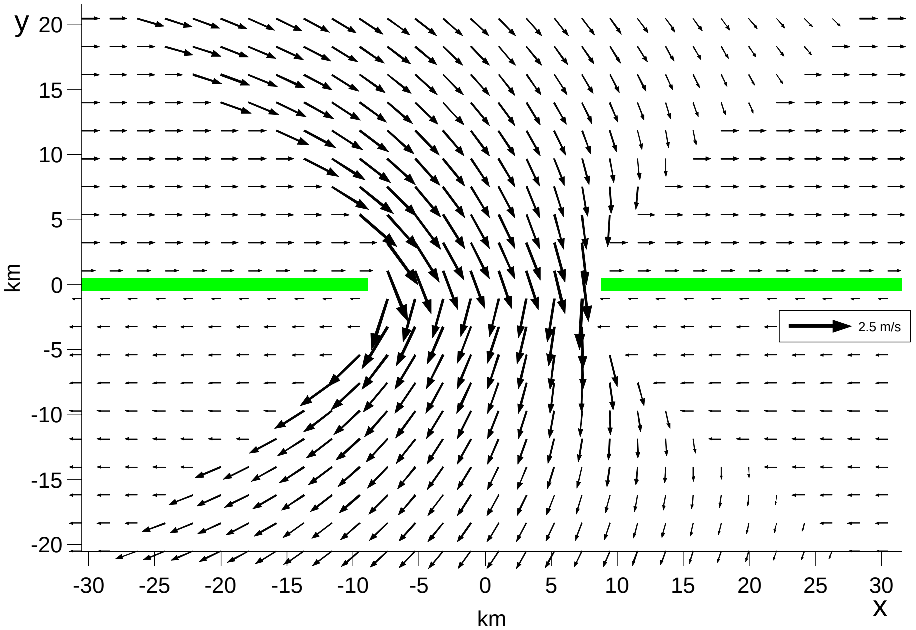

Figure 4: Sketch of the idealized current field with the BC superimposed. In this figure $C_1 = 0.7$, $C_2 = 0.5$, $t = 0$ and $\delta = 0$. We measure C_1, C_2 in m/s and t in seconds.

(0.1-0.7 m/s), the lengths L_1 and L_2 alters. If we keep $C_1 > C_2$, L_1 would change more than L_2. While L_2 would retain a value near 13 km, L_1 would change by several kilometers. By symmetry $L_1 = L_2$ for $C_1 = C_2$. If we alter the smoothing length R, we would also alter P. The intention of the smoothing length is only to avoid a discontinuity in the middle of the aperture. Keeping a reasonable size of R, we will generate a P with nearly same extension and distribution. For the simulations represented in this paper we have smoothed the BC by setting $R = 1$ km.

4.1 Results from the idealized model

The numerical time step, particle trajectories, particles released from a source, cluster simulations and estimation of the exchange parameter P (equation (8)) will be studied and represented in this section.

In figure 5 and 6 we demonstrate the importance of choosing an appropriate time step for the idealized model. The position of initial release for the particles is marked by a ×. Particles were divided into two categories, sensitive and non sensitive, according to their reaction of decreasing/increasing the numerical time step. Figure 5 shows a non sensitive particle, which has reliable trajectories even for "large" time steps. Figure 6 shows a sensitive particle. For the sensitive particle it is crucial to integrate with a small time step. Non sensitive particles are characterized by stability to perturbation in the phase $\delta \pm \Delta\delta$ of the current field or equivalent perturbation in the initial time of release $t_0 \pm \Delta t_0$. This means that for the particle in figure 5, released in the current field with a perturbation in phase, the particle would still leave through the aperture and remain on this new side for the rest of the simulation. Sensitive particles however are restricted to this small area spanned by the perturbations $[\delta - \Delta\delta, \delta + \Delta\delta]$ (or equivalent $[t_0 - \Delta t_0), t_0 + \Delta t_0])$. In this area, in the phase domain or time domain, we will have both particles that remain in their initial region and those who change region (see figure 2). The phase δ and the time t_0 in these expressions are not independent the position of release (the particles in figure 5 and 6 are released in the same position). In order to obtain a high degree of accuracy in the entire field we used a small time step set by the accuracy of the sensitive particles. This involves rather ineffective integration of the non sensitive particles but sufficient integration for sensitive particles. However, the chosen time step did not increase the computational cost to an unacceptable level.

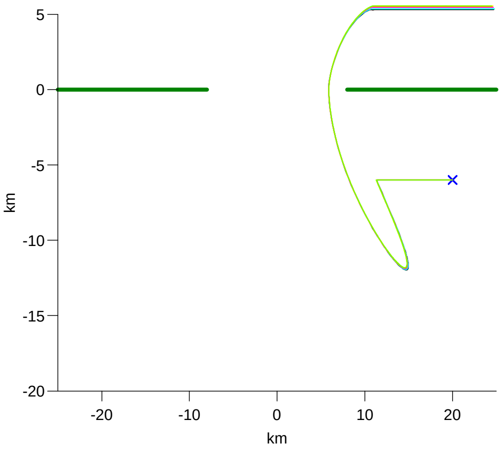

Figure 5: Convergence of particle trajectory for a non sensitive particle. Six particles are released under identical conditions, dropped in position $(20, -6)$ with different time step ($\Delta t = 0.105, 0.085, 0.065, 0.045, 0.025$ and 0.005 hours) used in the numerical integration. In this figure all six trajectories are indistinguishable.. The total simulation time for each trajectory is within 29.17 ± 0.14 hours. In this figure $C_1 = 0.5$, $C_2 = 0.2$, $t_0 = 0$ and $\delta = 0$, see model description section 4.

For the numerical simulations in this idealized model, a time step $\Delta t = 0.025$ hours was used to ensure reliable trajectories of the particles released. If not elsewhere mentioned the particles are released at simulation start $t = 0$.

Particle trajectories

The current field is completely periodical and particles released on the same spot separated by the tidal period T will therefore have identical trajectories. For particles released within this period the trajectories can differ greatly.

In figure 7, six particles are released on the same spot uniformly separated by only $T/200$ hours. The first three particles will remain in their initial region, while the last three change region. The figure shows that particles changing region do not necessary leave through the aperture within the first outgoing current, that the trajectories of each particle is unique and that the time spent within the time-dependent current differs greatly.

Particles released from a source

The simulation in figure 7 can be regarded as a source releasing 6 particles uniformly during a time interval of 0.31 hours. Here we will extend this interval and study the patterns of the particles released from this source. A total number of 2000 particles are released over a time interval of 100 hours, each separated by 0.05 hours. Figure 8 shows the result in this case.

Particles leaving the time-dependent current will build up patterns, like the loops in region 1 and strings in region 2. The 6 particles shown in figure 7 capture the switch between particles that will build up strings (remain in their initial region) and those that will build up loops (changing region). The particle distribution in each loop (and in each string) will be identical if the separation time between each particle released from the source is proportional the period T and if we wait until a steady state is obtained. During the simulation no two particles will enter the flow through the aperture under the same conditions, hence each particle has unique trajectories. If particles were released every T/M hour (M =number of particles),

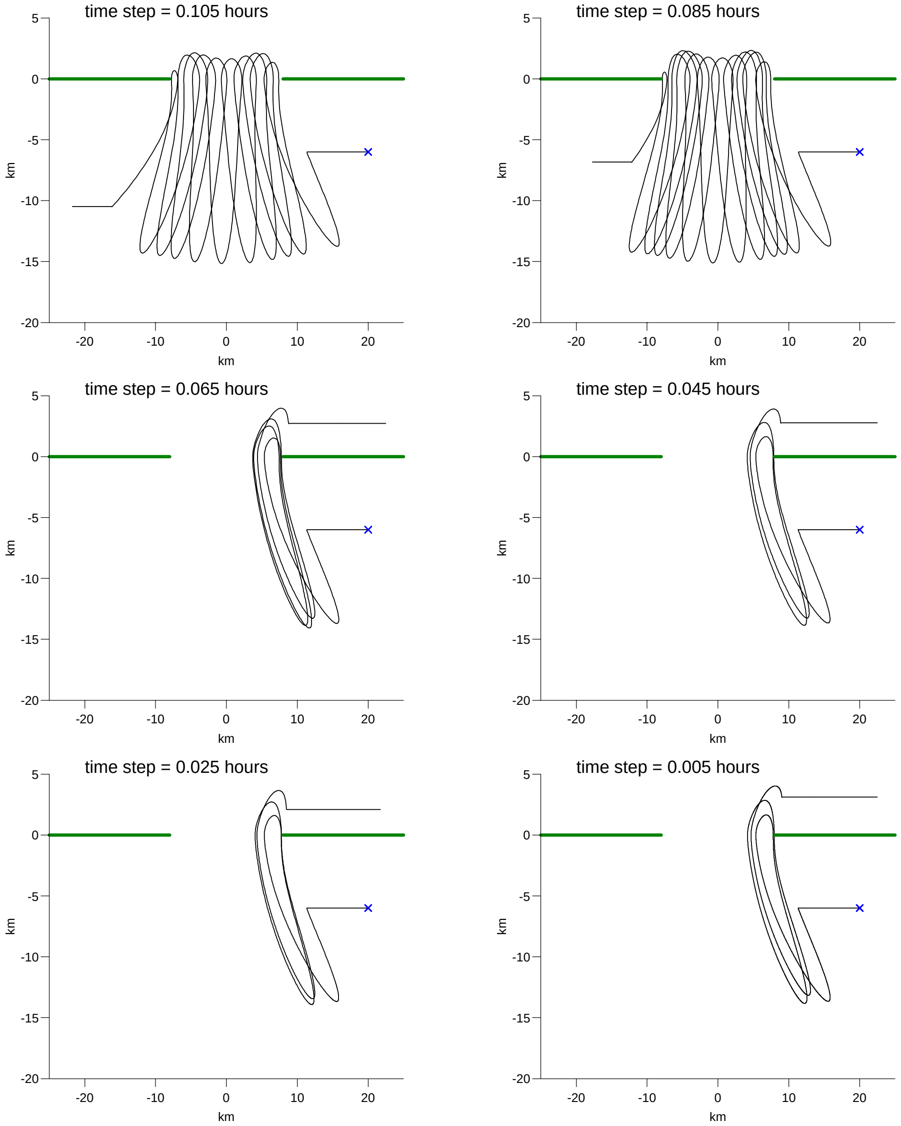

Figure 6: Convergence of particle trajectory for a sensitive particle dropped in position $(20, -6)$. The particle is released under identical conditions and the particle trajectory is calculated with decreasing numerical time step Δt. The total simulation time varies from $55.95 (\Delta t = 0.025)$ to $169.66 (\Delta t = 0.085)$ hours. In these figures $C_1 = 0.5$, $C_2 = 0.2$, $t_0 = 0$ and $\delta = 16.8\pi/100$, see model description in section 4.

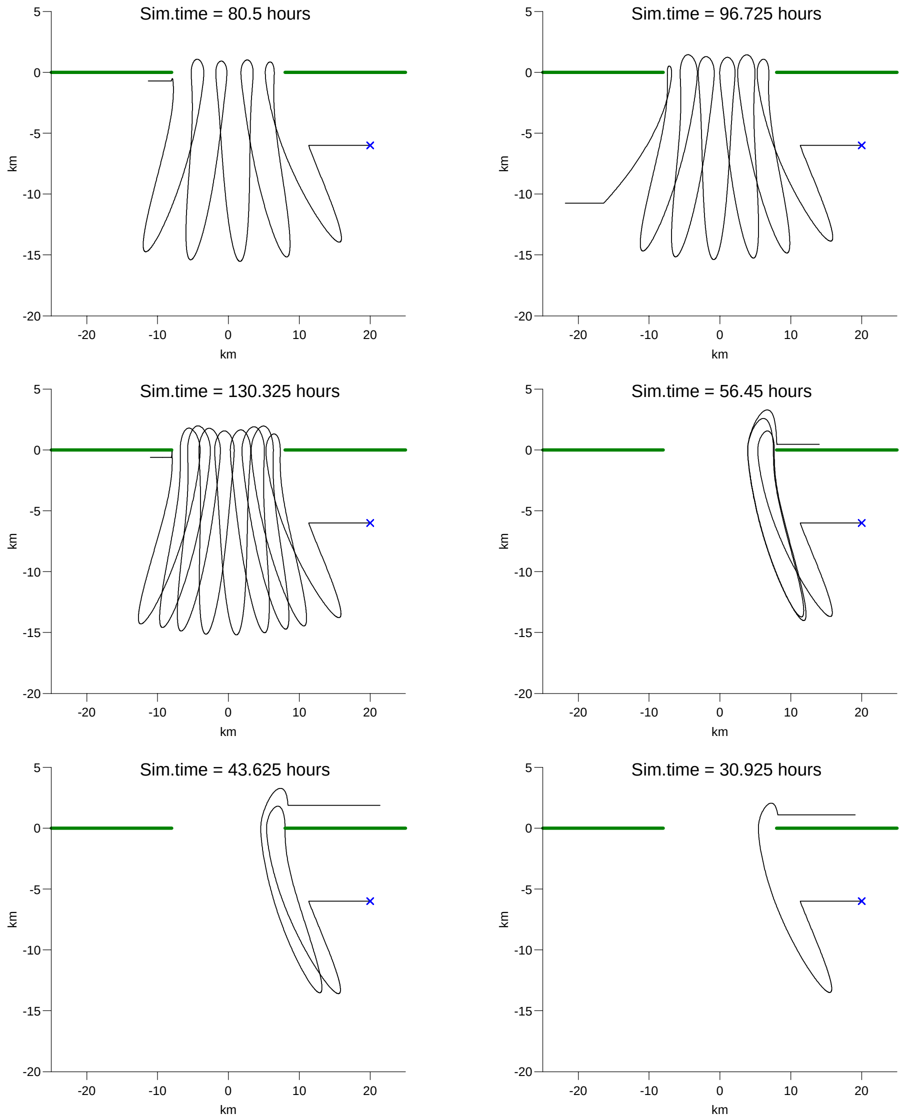

Figure 7: The particles are released in coordinate (20,-6). The phase δ is $\frac{\pi}{5}$, $C_1 = 0.5$, $C_2 = 0.2$ and the particles are released at respectively $t = 0, 3600T/200, \ldots, 3600(5T)/200$ ordered left-right top-bottom. Each simulation is stopped 7.5 hours after the particle leaves the time-dependent current. The time spent within the time-dependent current equals the simulation time (Sim.time) subtracted 19.525 hours.

particles separated by the period T will follow the same trajectories. These particles leaving the time-dependent current will therefore build up identical clusters, separated by the length $|\vec{U_1}| \cdot T$ and $|\vec{U_2}| \cdot T$ in respectively region 1 and region 2. Most of the particles in these clusters can be traced to particles released from the source within the same period. However, some particles can remain in the time-dependent current for quite some time, as seen e.g. in figure 7 left middle panel. Such particles will therefore leave the time-dependent current together with particles descended from a later release. Steady state in this context is therefore obtained when all the particles from the first period have left the time-dependent current.

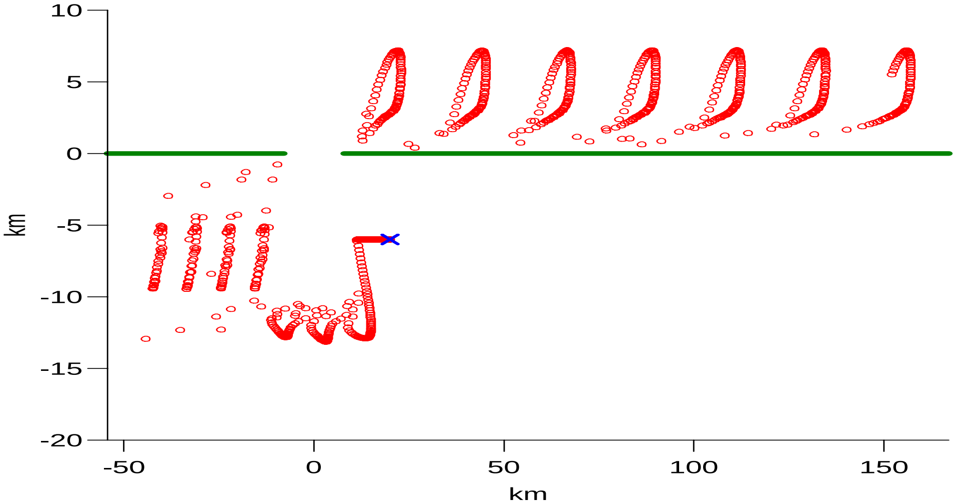

Figure 8: 2000 particles (circles) released, each with 0.05 hours separation, from a source located in coordinate (20,-6). The phase δ is 0, $C_1 = 0.5$, $C_2 = 0.2$. Total simulated time is 100 hours.

Cluster release and estimation of the exchange parameter P

A cluster of particles with an idealistic shape is released. The cluster consist of 5649 particles, separated by 0.1 km in the x-direction and 0.5 km in the y-direction, and has the shape of a square with upper left corner in coordinate $(20, -1)$ and lower right corner in $(48, -11)$. In this simulation the phase δ is 0, $C_1 = 0.5$, $C_2 = 0.2$. Simulation of 300 hours drift ensured that all particles had left the time-dependent current. At end time we found 1916 particles in region 2 and 3733 in region 1.

In figure 9 we have depicted the exchange parameter P for the region near the aperture. The exchange parameter is calculated with a spatial resolution of 500 meters. In each calculation point a total of 995 particles were uniformly released during a time interval $2T$. The exchange parameter will be independent the initial state of flow if we release many particles during a time interval $T_{sim} >> T$ or if we release many particles during whole periods of T.

We can use the exchange parameter to predict the transport of a cluster. For example the described square-cluster can be represented as fictive sources along a line in the $y-$direction from coordinate (20,-1) to coordinate (20,-11). If we estimate P to be a linear function of y using just the values of P shown in figure 9 from coordinate (20,-1) and (20,-11), 3630 particles of the cluster was predicted to change region. An improved result was obtained by using the resolution of P from figure 9 along a line in the $y-$direction from coordinate (20,-1) till coordinate (20,-11). The amount of particles changing region with this technique was estimated to be 3727.

The ideal shape of the cluster ensures the good estimate. The cluster can easily be represented by sources releasing particles during a time interval $2T$. The amount of particles released from each of the fictive sources is multiplied by an estimate of P for the same

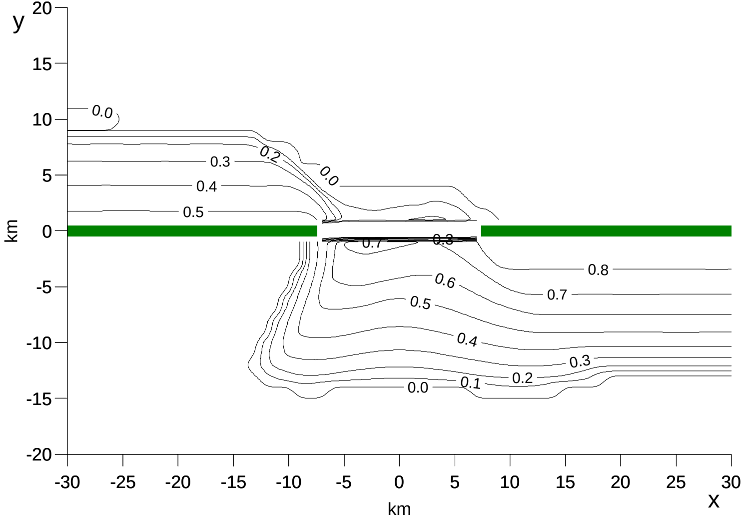

Figure 9: Contour lines for the exchange parameter P with 0.2 separation near the aperture for $C_1 = 0.5$, $C_2 = 0.2$ (idealized model). Note, P is not defined for $y = 0$.

position, and by addition of this value from all the sources representing the cluster we obtained the prediction represented. This technique gives good estimates for clusters which can be represented by s sources releasing over hole tidal periods or over a time intervals $T_s >> T$. These restrictions are necessary to ensure that the transport is not dependent too heavily on the initial state of the flow.

5 A realistic model

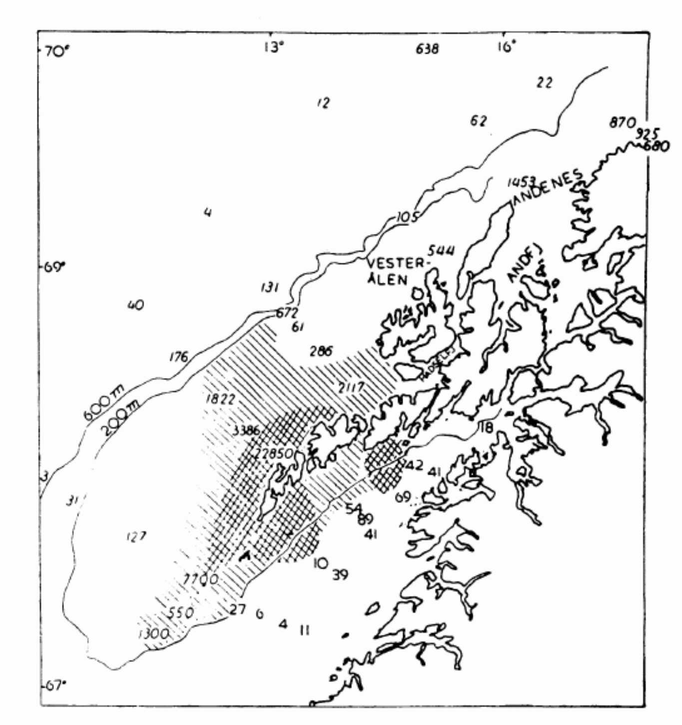

Figure 10: Distribution of cod eggs in Lofoten 4-5 April 1951. Crosshatched: 1000 – 6000 eggs/m^2 Hatched: 100 – 1000 eggs/m^2. After Wiborg (1952).

The Norwegian directorate of fisheries studied the amount of eggs and spawn in the North-

Norwegian coastal waters during spring 1950 and 1951. Figure 10 shows the distribution of cod eggs during spring 1951, taken from Wiborg (1952). We believe that most of the eggs found on the outer shelf descend from the most significant spawning area located in the northwestern part of Vestfjorden. However, Wiborg keep the possibility that the cod also has major spawning-areas on the outer shelf. He doubted that a significant amount off eggs were transported from Vestfjorden to the banks outside Lofoten. We will study the trajectories from particles released in Vestfjorden to see whether a large amount of cod eggs on the outer shelf may descend from spawning in Vestfjorden.

The numerical tracking algorithm for this region is named *the Lofoten model* to make a distinction from the idealized model. The time step used in this simulations was found by investigating several paths from particles released in different position and in different times. The time step used, $\Delta t = 0.0125$ hours, was then chosen by the most sensitive particle, see the discussion in section 4.1. Subsection 5.1 shows particles which are transported only due to the periodical tidal current. In subsection 5.2 a background current is added to simulate the general circulation. Section 6 shows the effect of the random-walk method.

5.1 Trajectories of single particles

The trajectories of particles released in Moskstraumen will be sensitive to their initial time and position of release. Identical trajectories from particles released at the same spot in different times are naturally found separated by the tidal period T. Figures 11-13 show a selection of some typical trajectories from this area. Single particles were released at $t = 0$ and 60 hours drift were simulated.

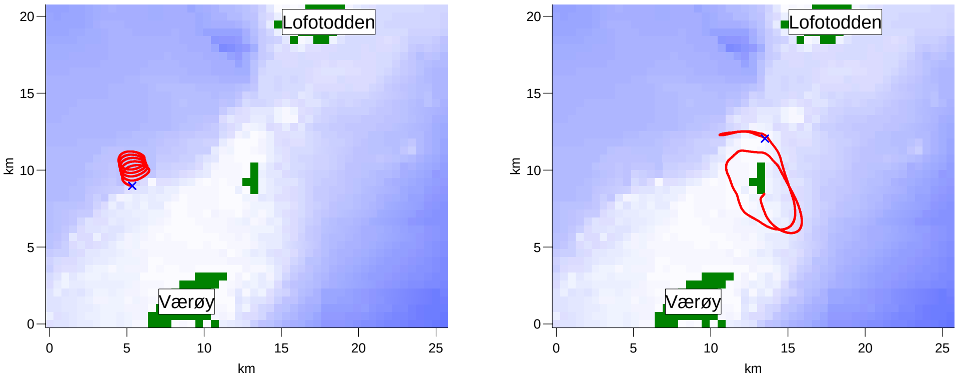

Figure 11: Left panel: Particle released in coordinate $(5.5, 9)$ demonstrate typical local elliptic motion in distance from the small island Mosken (located in the middle of Lofotodden and Værøy). Right panel: Particle released in coordinate $(13.5, 12)$ shows the deadlocking, beaching of particles that enters a dry grid.

Figure 11 left panel shows one particle with local elliptic motion, released in distance and west of Mosken. The clockwise motion agrees well with the rotation of the current vector described in appendix A and depicted in figure 22. This local elliptic motion is typical for particles released in distance from the sounds. Right panel demonstrate beaching of a single particle. The particle was beached after 27.74 hours and will remain on the small islands Mosken. Figure 12 shows the oscillatory nature of the flow. The particle in left panel shows typical local oscillatory, while the oscillation of the particle on right panel is not restricted to such a small area. Figure 13 illustrate the sensitivity of drop-position and the forcing of complex topography. Left panel shows a particle that loops around Mosken. The drop position is changed by 100 meters in the x-direction for the particle on the right panel.

The particle trajectories show that the tidal excursion of Moskstraumen is capable of transporting eggs and spawns from Vestfjorden to the outer shelf. The strong current is

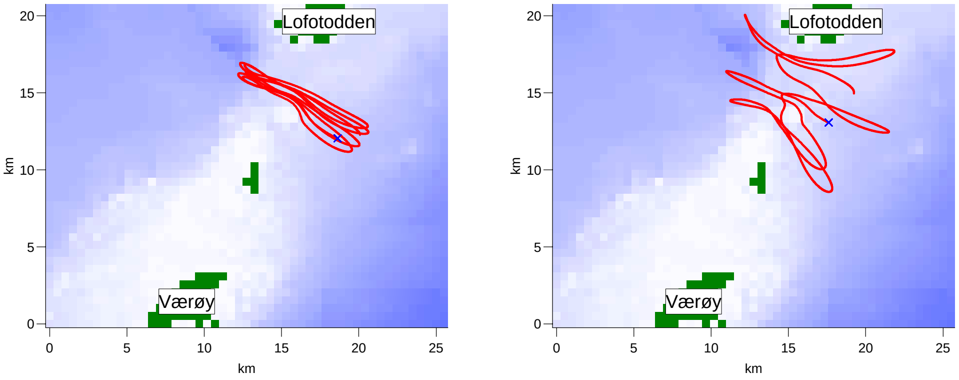

Figure 12: Left panel: Particle released in coordinate $(18.5, 12)$ shows local oscillatory motion. Right panel: Particle released in coordinate $(17.5, 13)$ shows oscillatory motion with more complex trajectory.

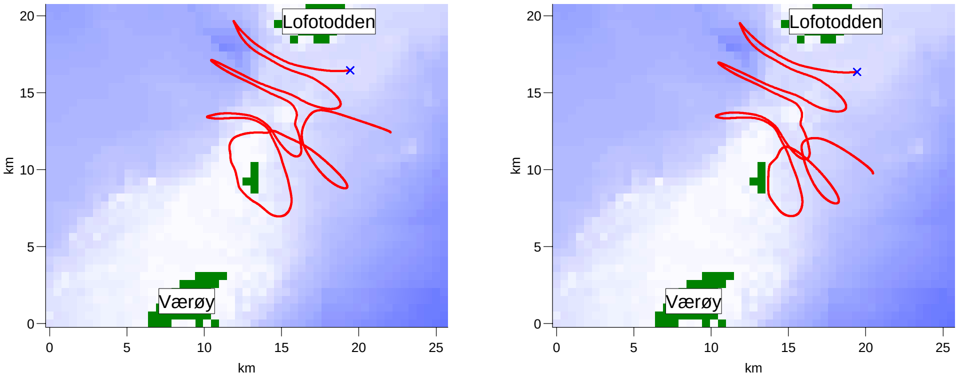

Figure 13: Left panel: Particle released in coordinate $(19.3, 16.2)$. Right panel: Particle released in coordinate $(19.3, 16.3)$. The particles demonstrate forcing of topography and the sensitivity in drop position.

restricted to a thin band from Værøy to Lofotodden. Typical trajectories are: local elliptic motion outside this band and more complex oscillatory motion from particles released inside. Eggs and spawns from the north-west part of Vestfjorden must therefore be transported close to the tip of Lofotodden if Moskstraumen should be able to capture them.

Motion of a cluster of particles

A cluster of particles was released in a region near Lofotodden. Figure 14 left panel shows the initial position of this cluster, which is made up by 313 particles, shaped in a circle with radius 2 km.

The drifting cluster is captured by Moskstraumen, and figure 15 shows the position of each particle after $6, 12, 18$ and 24 hours. Only 5 particles were beached after 24 hours, of which 3 were beached at the small island Sörholmen (coordinate $14.5, 19$) and two at the island Rødøy (coordinate $15.5, 18$). Rødøy is merged with Lofotodden due to the grid resolution used here. We increased the simulation time to ensure that a majority of the cluster did not experience a “mathematical beach”. Figure 14 right panel shows the end position of this cluster after 100 hours. Moskstraumen has dispersed this cluster. The current field forced by the small island Mosken will contribute strongly in this dispersion. Of the total 313 particles released 10 beached near Lofotodden and 32 at Mosken. Moskstraumen transports a large part of the cluster in between the inner and outer shelf, and the cluster is strongly stretched and reshaped. The mechanism is the same as in the idealized model, a periodical current.

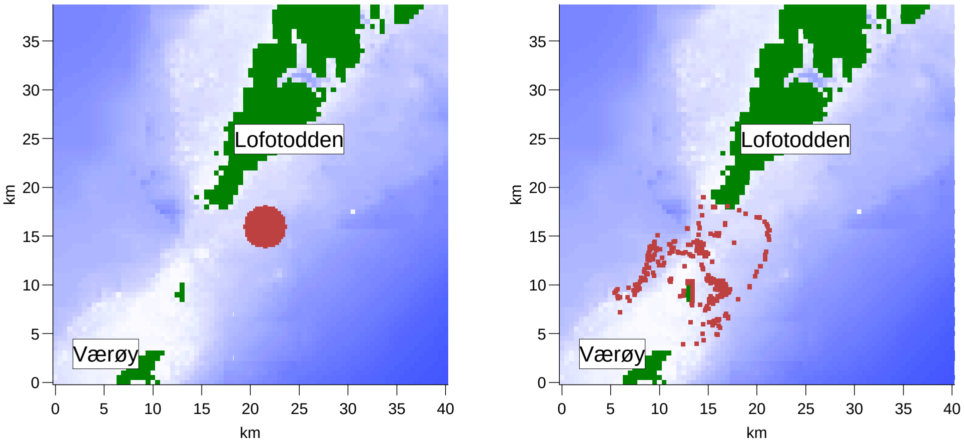

Figure 14: Left panel: Initial drop position of a circular cluster made up by 313 particles with a radius of 2 km. The center of the cluster is located in coordinate $(21.5, 16.5)$. Right panel: End position of particles after 100 hours drift in the tide.

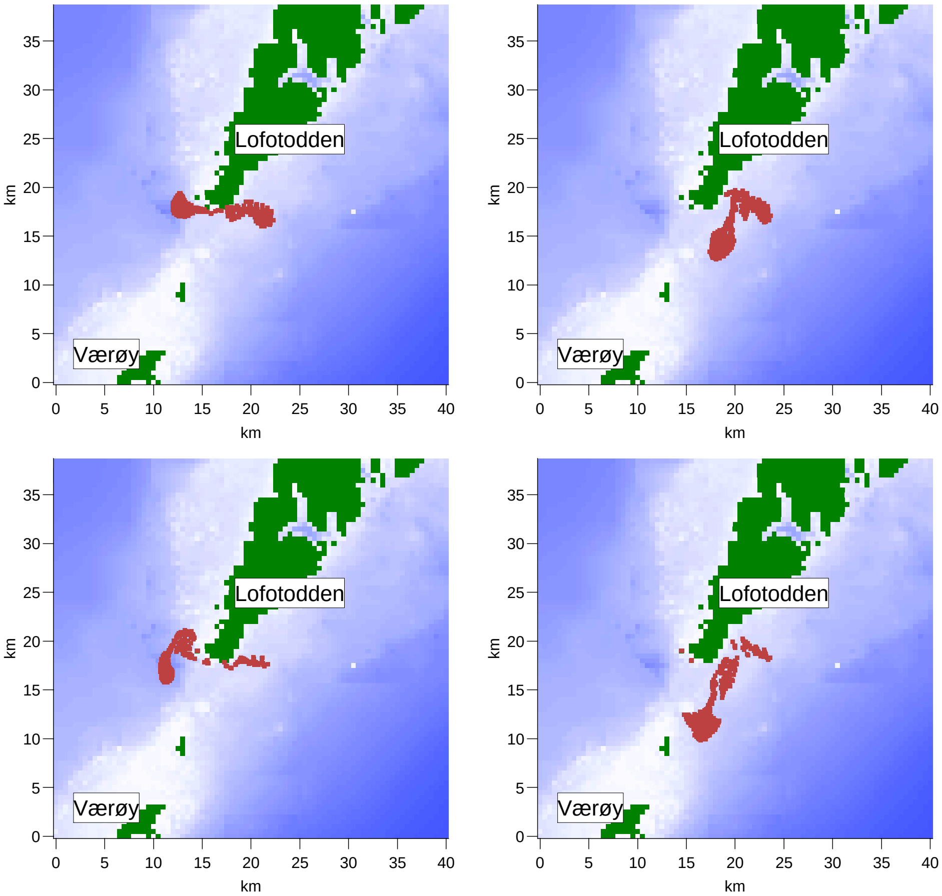

Figure 15: Drift and dispersion of the cluster due to the tide. The simulated drift is for 6, 12 (upper panels), 18 and 24 hours (lower panels).

The complex drift of particles released, illustrated by figure 11-15 is due to gradients in the Eulerian current field. We also placed the initial cluster 4 km further east, in this case no particles would enter the outer shelf and the cluster would move in an elliptic motion and still be cluster-shaped after 100 hours simulation (plots not shown here).

5.2 Effect of background current (BC)

We have designed idealized BC in order to simulate the general circulation introduced by the Norwegian Coastal Current in the area. One branch of this coastal current enters Vestfjorden on the south-east side and exits along the Lofoten archipelago on the west side, Furnes and Sundby (1980). In this section we will study drift of particles with additional BC. We simply add to the oscillatory tidal current a constant northward shelf current on the west side of the Lofoten island and a constant southward current inside the Lofoten islands. Figure 16 indicates the location and the separation zone between the two branches of the steady current. If not elsewhere mentioned we have used a constant northward depth mean current of 0.3 m/s and a constant southward depth mean current 0.1 m/s.

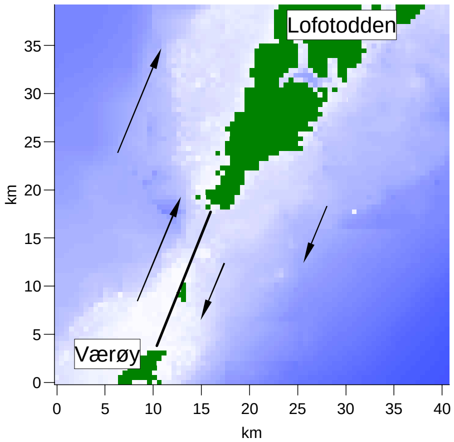

Figure 16: The structure of the idealized background currents. The arrows shows the current direction, and the solid line the separation zone between the two branches of the current.

The addition of BC will dramatically alter the trajectories of particles released. To avoid steady drift towards or from islands and land BC were only added two grid-points from dry points (zero depth).

Particle trajectories

Figure 17 shows two typical trajectories of single particles. The particle on the left panel is captured by Moskstraumen and transported towards the northward BC. Although being trapped in the strong current for several periods, the particle never enters the northward BC. On the right panel we have released a particle at the same spot, but with a delay of 0.1 hour. This particle enters the northward BC and is transported northward. These two particles demonstrate the change in particle trajectories due to a short phase disturbance. Picture a source placed at coordinate $(25.5, 23)$, the first particle is one of the last particles that will leave south-east of Værøy, while the second particle is one of the first particles entering the outer shelf during the first tidal period. The same situation is depicted for the idealized model in figure 7.

In our model eggs found on the outer shelf can only descend from Vestfjorden if they once were transported close to the tip of Lofotodden. For this particular run the crucial border is within approximately 5 km east of the tip of Lofotodden (fig. 18). This result is

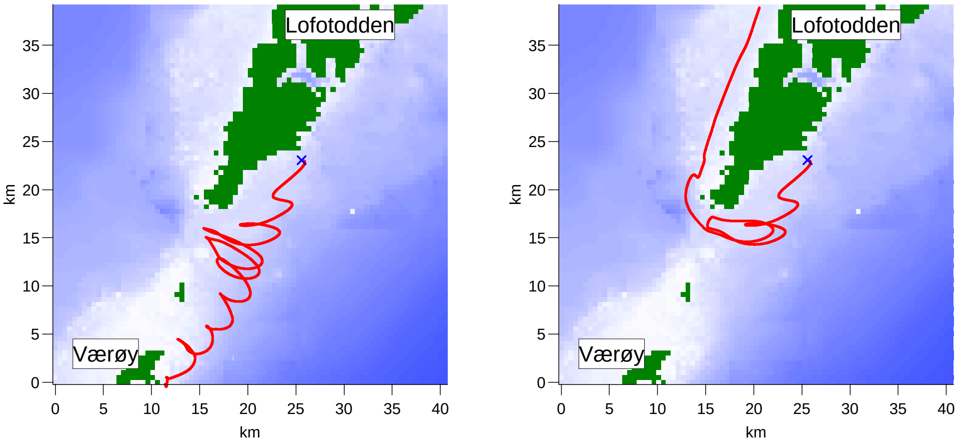

Figure 17: Two particles released in coordinate (25.5, 23), separated by 0.1 hour. Left panel: Particle released at $t = 7.1$ hours with 122.9 hours drift. Right panel: Particle released at $t = 7.2$ hours with 60 hours drift.

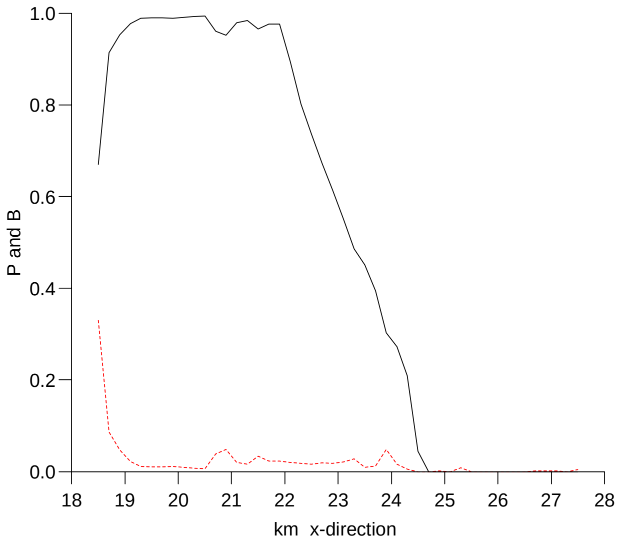

Figure 18: The exchange parameter calculated along a line from coordinate (18.5,18.25) to (28,18.25) with the sources separated by 200 meters. 1000 particles were uniformly released by each source during a time interval equal to the tidal period. The simulation of the particles was stopped when all particles had either *changed region*, beached or left south-east of Værøy. The dotted line shows B defined in equation 9 for the same area. Since most of the beached particles will be sticked to the tip of Lofoten (the separation zone) they are counted as particles that do not change region. The particles being transported south-east of Værøy are stopped, so the fact that particles may also enter the outer shelf south of Værøy is not considered.

strongly dependent of our chose of BC. We calculated the exchange parameter for different BC strengths and defined the beach parameter to be

$$B = \frac{Number\ of\ particles\ beached}{Total\ number\ of\ particles\ dropped\ in\ position\ x{,}y} \tag{9}$$

The beach parameter is defined to quantify the amount of beached particles and to ensure reliability in the representation of P. The beached particles were counted as particles unable to change region. The effect of increasing/decreasing the northward BC (within 0.2-0.5 m/s) does not alter much the shape and extension of the exchange parameter shown in figure 18. Increasing the southward BC gives a more linear P, with $P = 0$ at approximately $x = 24$ km.

During these simulations, with the simplified BC and without diffusion, there is a possibility for particles to be trapped within Moskstraumen. From figure 18, and other simulations of P and B, beaching was only considered a problem when particles were released very close to land ($x \approx 18.5$).

Motion of a cluster of particles

Figure 19 is one example of drift and dispersion of a cluster with BC. The initial position, shape and size of the cluster are as described and illustrated in figure 14 left panel. In this simulation beaching of particles is not considered a problem. After 24 hours only 12 particles beached. They were all found deadlocked on the island Sörholmen. A great amount of

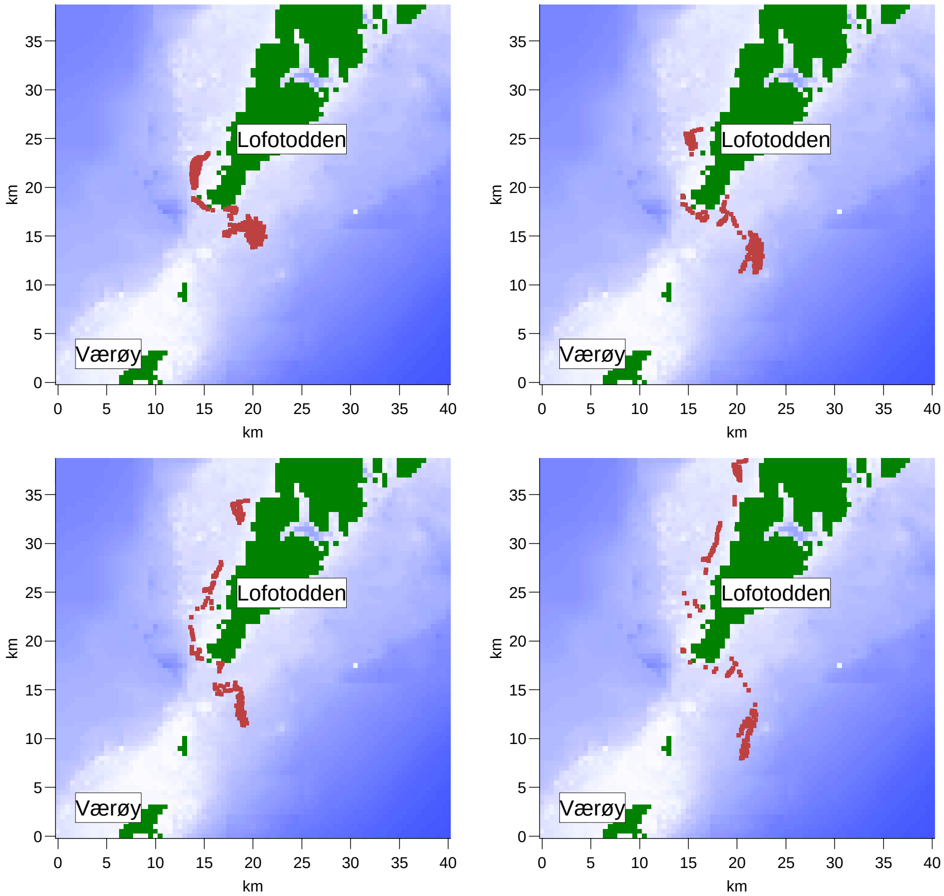

Figure 19: Drift and dispersion of the cluster with the addition of BC. The initial position of the cluster is shown in figure 14 left panel. The simulated drift is for 6, 12 (upper panels), 18 and 24 hours (lower panels).

particles are transported in a northward direction in this simulation. Approximately thirty percent of the cluster is transported through the sound between Mosken and Lofotodden and transported in a northward direction already after 12 hours. Moskstraumen transport the particles in between Vestfjorden and the outer shelf and many particles are captured by the northward *BC*. Of the total 313 particles released in Vestfjorden, 244 changed permanently region and 57 left the model domain southward on the inner shelf (the remaining 12 were beached).

6 Diffusion simulated by random-walk

The random-walk approach enables simulation of diffusion processes without solving the advection diffusion equation. We used the random-walk method mainly to simulate small scale homogeneous turbulence, although several other options are possible. The results presented here are with a constant diffusion coefficient, but simulations where also made where the strength of the diffusion was related to the eddy viscosity (current shear) or to the tidal speed.

The random-walk method alone performed, according to the analytical results presented in section 3, as a generator of Fickian diffusion with an effective diffusivity coefficient $K \approx K_h$. An increase in the amount of particles released will improve the performance of the random-walk method as a simulator of diffusion, see e.g. Furnes (1994) and/or Hunter (1980). This improvement will naturally increase the computational cost.

We used the forth order Runge-Kutta method for the numerical integration of equation (3). The random-walk method displace each particle a length D each time step, so we can no longer use a mulitstep method (Adam-Moulton).

Figure 20 is a repetition of the simulation in subsection 5.2 figure 19 where we have used the random-walk method to simulate small scale turbulence. As expected horizontal small scale turbulence will smear out the cluster shapes but the general drift pattern is preserved, as seen from the figures 19 and 20. A moderate diffusion coefficient have been used to demonstrate the effect of the random-walk method. More data of the strength of the small scale turbulence is needed to construct a more realistic diffusion coefficient.

7 Concluding remarks

A particle tracking algorithm is implemented for the Lofoten region. Trajectories are computed from data obtained by a harmonic analysis of the current times series modeled in Gjevik et al. (1997). The tracking of particles from Vestfjorden demonstrate that the tidal current in Moskstraumen combined with the steady background currents (*BC*) in this region is an important mechanism for the water exchange between Vestfjorden and the outer shelf. This mechanism may explain why a large amount of cod eggs in some cases are found on the outer shelf, despite the fact that the important spawning area is located inside Vestfjorden, close to the Lofoten archipelago.

An idealized model was developed to demonstrate the exchange mechanism. This idealized model was used to demonstrate the importance of finding a suitable time step for the numerical integration. The idealized model inhibit the current profile in Moskstraumen, and it is justified through the simulations. To quantify the exchange an *Exchange Parameter*, measuring the water exchange in different positions, was constructed.

With our constructed *BC* in the Lofoten model the eggs found on the outer shelf, which initially descend from Vestfjorden, must once have been transported by the *BC* within approximately 5 km east of Lofotodden. This to enable the tidal excursion in Moskstraumen to transport them into the northward directed current. Within this 5 km border the *Exchange*

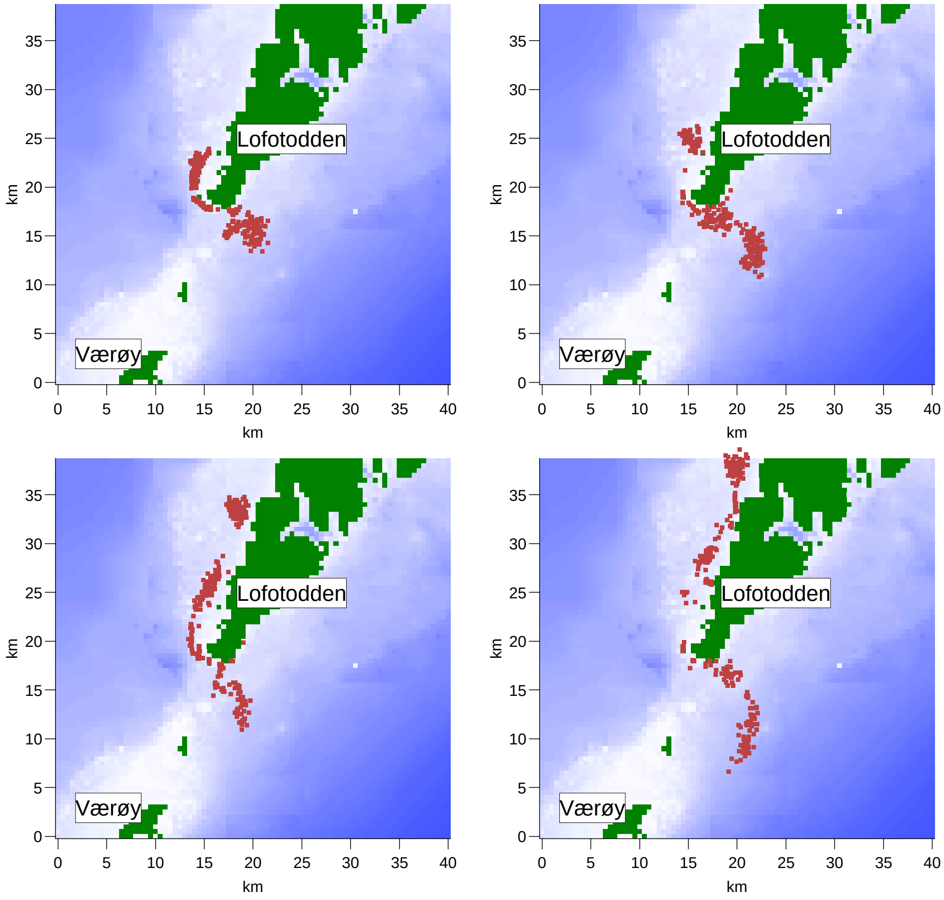

Figure 20: Drift and dispersion of the cluster with the addition of *BC* and diffusion. The simulated drift is for 6, 12 (upper panels), 18 and 24 hours (lower panels). The diffusion coefficient K_h is 10 $\mathrm{m}^2\mathrm{s}^{-1}$.

Parameter revealed that the likelihood for a particle leaving for the outer shelf may be as large as one, and such a large exchange may exist within a large part of the border.

In this model Moskstraumen is considered the only outlet between Vestfjorden and the outer shelf. Other outlets, like south of Værøy and the straits in the northern part of the Lofoten archipelago, are also important for the water exchange between Vestfjorden and the open sea. A similar mechanism for water exchange (tidal current combined with BC) will also occur in these regions. Since the other straits in the northern part are long and narrow and combined with an expected reduction in tidal excursion the pumping of the tide will be less efficient compared to that in Moskstraumen. More realistic modeling of the BC are needed to quantify this exchange.

We deadlock particles when they encountered the extension of a dry grid point (zero depth). The contour of the grid point was not considered and current shifts could not transport the particles back into the simulation. Beaching was only considered a problem in the calculation of P when the calculation point was within one grid cell distance from Lofotodden. With our treatment of beached particles, we decided to add BC only in a distance of two grid points from dry grid points. This to prevent steady drift from or towards land.

We implemented a random-walk method to simulate small scale turbulent diffusion. This is an effective and computationally cheap approach. The method is well known for modeling a diffusion process, but like in the advection-diffusion equation its correctness is strongly dependent on the use of an appropriate diffusion coefficient model.

Our basis tidal model neglect the effect of dispersion due to residual currents. A nonlinear (3D) model and better knowledge about BC are necessary to make more accurate and reliable estimates of the particle trajectories. In our model the periodical nature of the tidal current enables a study of particle trajectories from only a small initial data subset. Expanding the model with nonlinear terms leads to different and tougher computation of trajectories. The particle tracking algorithm must then be implemented together with the nonlinear model. Particles initial positions and time of release must be pre-declared, and this will most likely lead to a computationally costly nonlinear model being recalculated several times. The complexity and chaos of the trajectories may even force a smaller time step in the nonlinear model.

Trajectories from particles released in Moskstraumen were very site and time dependent, and the tidal current field alone lead to strong dispersion of clusters released due to the strong gradients in the current field. An approach using the theory from chaotic motion (Hamilton) for this region was made, but the divergence of the current field combined with limiting the scope of this paper suggested this topic as a prospective future study.

Acknowledgement

I am indebted to Prof. B. Gjevik for reading the manuscript and making many suggestions and corrections. This work has also received support from The Research Council of Norway through project funding (MAREMI).

A Calculation of the major and minor axis, eccentricity and rotation

The components of the M_2 depth mean current velocity for fixed coordinate x, y are written

$$\hat{u} = U_e \cos(\omega t - g_e) \tag{10}$$

$$\hat{v} = V_n \cos(\omega t - g_n) \tag{11}$$

Here (U_e, V_e) denotes the amplitudes for this coordinate, ω the angular velocity and g_e, g_n phases where the terms (δ_u, δ_v) and χ from equation 1 and 2 are combined. The trace of the tip of the current vector $\vec{s} = \sqrt{\hat{u}^2 + \hat{v}^2}\,\vec{i_r}$, where $\vec{i_r}$ is the radial unit vector, is an ellipse as shown in figure 21.

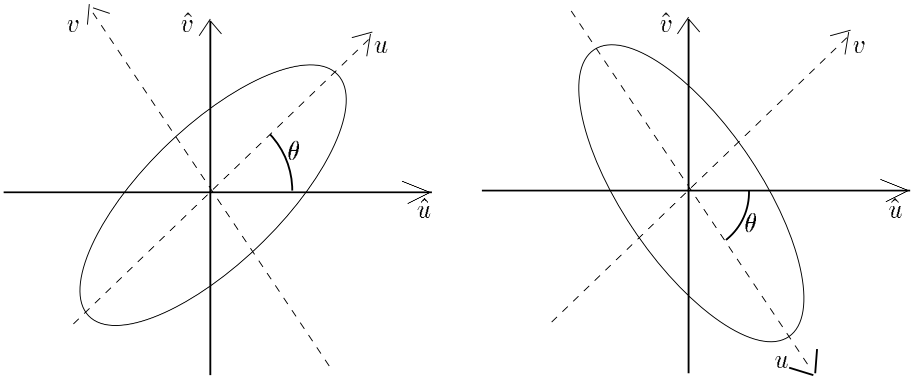

Figure 21: Two possible ellipses. The revolved angle θ is chosen so that the major axis coincide with u.

A new coordinate system is drawn onto figure 21 revolved by an angle θ from the original system. The new axes coincide with major and minor axis of the ellipse. The components of the current in this new coordinate system are

$$\begin{aligned} u &= \hat{u}\cos\theta + \hat{v}\sin\theta && (12) \\ v &= -\hat{u}\sin\theta + \hat{v}\cos\theta && (13) \end{aligned}$$

We rewrite equation (12) and (13)

$$\begin{aligned} u &= A\sin(\omega t - \zeta) && (14) \\ v &= B\cos(\omega t - \zeta) && (15) \end{aligned}$$

and get the expression for the amplitudes

$$\begin{aligned} A &= \sqrt{(A_1\cos\theta + A_2\sin\theta)^2 + (B_1\cos\theta + B_2\sin\theta)^2} \\ B &= \sqrt{(A_1\sin\theta - A_2\cos\theta)^2 + (B_1\sin\theta - B_2\cos\theta)^2} \end{aligned}$$

here

$$\begin{aligned} A_1 = U_e\sin(g_e) \quad &, \quad A_2 = V_n\sin(g_e) \\ B_1 = U_e\cos(g_e) \quad &, \quad B_2 = U_e\cos(g_n) \end{aligned}$$

The major axis is defined as $2A$ and the minor $2B$. The revolved angle θ is determined by equation

$$\tan 2\theta = \frac{2(A_1A_2 + B_1B_2)}{A_1^2 - A_2^2 + B_1^2 - B_2^2}$$

We force the major axis to coincide with u, if necessary replacing θ with $\theta = \theta \pm \frac{\pi}{2}$.

The rotation of the current vector is determined by expression

$$R = u(t_0) \cdot \frac{dv(t_0)}{dt}$$

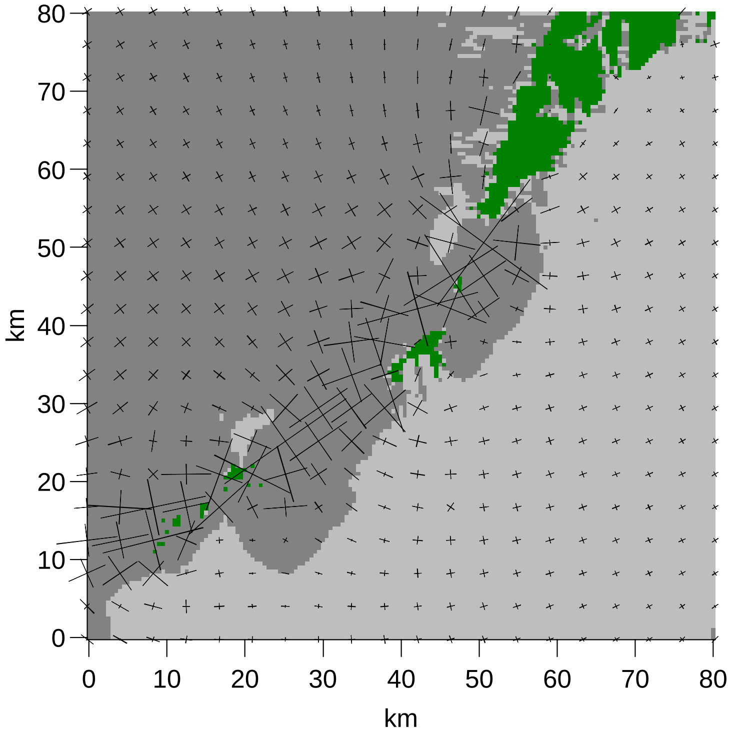

Figure 22: The rotation of the current vector. Bright shadowing depicts region with anti-clockwise rotation, darker shadowing depicts region with clockwise rotation. The crosses show the major and minor axis with a reduced resolution to avoid cluttering. The eccentricity calculated for this area ranges from [0.23 – 1.0) with common values near 1. Areas with low eccentricity is found near Værøy and Røst (Røst is the islands located near coordinate (20,20).

The time t_0 is chosen so that $u(t_0) \neq 0$. Then $R < 0$ is a clockwise rotation, $R > 0$ anti-clockwise. Figure 22 shows the rotation and the axis of the ellipses for a subdomain of the simulation in Gjevik et al. (1997). The dark-shadowed area is $R < 0$ a clockwise rotation, $R > 0$ in a brighter shadow.

The eccentricity e of the ellipses is defined

$$e = \sqrt{1 - \frac{B^2}{A^2}} \qquad 0 \leq e \leq 1$$

The larger eccentricity, the more elongate is the ellipse. If $e = 0$ then $A = B$ and the trace of the current vector S is a circle with radius A. With $B = 0$, the trace is a strait line with length $2A$.

References

Boyce, W. E., DiPrima, R. C., 1992. Elementary Differential Equations and Boundary Value Problems (5 ed.). John Wiley & Sons, Inc.

Ellertsen, B., Furnes, G. K., Solemdal, P., Sunby, S., 1980, 9-12 september. Influence of Wind Induced Currents on the Distribution of Cod Eggs and Zooplankton in Vestfjorden. In R. Sætre and M. Mork (Eds.), The Norwgian Coastal Current, Volume 2 of Proceedings from the Norwgian Coastal Current Symposium, Geilo, pp. 604–628. University of Bergen.

Elliott, A. J., 1986. Shear Diffusion and the Spread of Oil in the Surface Layers of the North Sea. *Deutche hydrographische Zeitscrift* 39, 113–137.

Elliott, A. J., Dale, A. C., Proctor, R., 1992. Modelling the Movement of Pollutants in the UK Shelf Seas. Marine Pollution Bulletin 24(12), 614–619.

Elliott, A. J., Hurford, N., Penn, C. J., 1986. Shear Diffusion and the Spreading of Oil Slicks. Marine Pollution Bulletin 17(7), 308–313.

Furnes, G. K., 1994. Discharges of Produced Water from Production Platforms in the North Sea. Technical Report R-064641, Norsk Hydro.

Furnes, G. K., Sundby, S., 1980, 9-12 september. Upwelling and Wind Induced Circulation in Vestfjorden. In R. Sætre and M. Mork (Eds.), *The Norwgian Coastal Current*, Volume 1 of *Proceedings from the Norwgian Coastal Current Symposium, Geilo*, pp. 152–177. University of Bergen.

Geyer, W. R., Signell, R. P., 1992. A Reassessment of the Role of Tidal Dispersion in Estuaries and Bays. Estuaries 15(2), 97–108.

Gjevik, B., 1996. Models of Drift and Dispersion in Tidal Flows. In J. Grue, B. Gjevik, and J. E. Weber (Eds.), *Waves and Nonlinear Processes in Hydrodynamics*, pp. 343–354. Kluwer Academic Publishers.

Gjevik, B., Moe, H., Ommundsen, A., 1997. Sources of the Maelstrom. Nature 388(28), 837–838.

Hunter, J. R., 1980. An Interactive Computer Model of Oil Slick Motion. In *Oceanology international 80*, pp. 42–50.

Hunter, J. R., 1987. The application of langrangian particle-tracking techniques to modelling of dispertion in the sea. In J. Noye (Ed.), *Numerical Modelling: Application to Marine Systems*, pp. 257–269. Elsevier Science Publisher B.V.

Milne-Thomson, L. M., 1968. *Theoretical Hydrodynamics* (5 ed.). Macmillan.

Proctor^1, R., Elliott, A. J., Flather, R. A., 1994. Forecast and Hindcast Simulations of the Braer Oil Spill. Marine Pollution Bulletin 28(4), 219–229.

Proctor^2, R., Flather, R. A., Elliott, A. J., 1994. Modelling Tides and Surface Drift in the Arabian Gulf- application to the Gulf Oil Spill. Continental Shelf Research 14(5), 531–545.

Ridderinkhof, H., Zimmerman, J. T. F., 1992. Chaotic Stirring in a Tidal System. Science 258(13/11), 1107–1111.

Turell, W. R., 1994. Modelling the *Braer* Oil Spill- A Retrospective View. Marine Pollution Bulletin 28(4), 211–218.

Wiborg, K. F., 1952. Forekomst av Egg og Yngel i Nordnorske Kyst- og Bankfarvann Våren 1959 og 1951. *Fiskeridirektorates Småskrifter* 1, 1–22.

Zimmerman, J. T. F., 1986. The Tidal Whirlpool: A Review of Horizontal Dispersion by Tidal and Residual currents. Netherlands Journal of Sea Research 20(2/3), 133–154.